Asian Journal of Applied Sciences



Asian Journal of Applied Sciences 7 (8): 685-695, 2014 ISSN 1996-3343 / DOI: 10.3923/ajaps.2014.685.695 © 2014 Knowledgia Review, Malaysia

Electronic Transport at Low Temperature in some Sandwiched Films

¹R. Ramanna, ¹P.J. Sadashivaiah, ¹T. Sankarappa, ²T. Sujatha, ¹J.S. Ashwajeet, ¹A.W. Manjunath and ¹Santosh Kori

¹Department of Physics, Gulbarga University, Gulbarga, 585 106, India

Corresponding Author: T. Sankarappa, Department of Physics, Gulbarga University, Gulbarga, 585 106, India

ABSTRACT

A series of sandwiched films in the configuration, Ni(100 nm)/Al(t)/Ni(100 nm); t = 10 nm, 20 nm,....., 100 nm (labeled as NAN1, NAN2,...., NAN10) were produced by thermal and electron beam gun evaporation techniques. The films were deposited onto the glass substrates held at 200°C, under high vacuum conditions in a Hindhivac coating unit. The structure, grain size and interplanar distances were probed by X-Ray Diffraction (XRD). The grain sizes obtained were in the order of few nanometers and decreased with increasing, t. Electrical resistivity in the temperature range from 4 to 300 K has been measured in an Oxford Instruments make resistivity measurement setup. The resistivity decreased nonlinearly and continuously with increasing temperature for the films NAN1, NAN3 and NAN7 similar to that of a semiconductor. Mott's small polaron hopping and variable range hopping models due to Mott and Greave have been employed to understand resistivity variation with temperature. In the remaining films resistivity decreased up to some temperature and increased thereafter. This indicated a kind of transition occurring in these films from Metallic to Semiconductor (MST). These results are significant as neither of the constituent layers in the present films is semiconducting by nature. The resistivity variation with temperature of some of these films has been analyzed using semi-classical conductivity model of Boltzman which incorporates quantum corrections in to it. It is for the first time that the sandwiched films of the present configuration have been investigated for structure and low temperature resistivity and data analyzed thoroughly.

Key words: Sandwich films, XRD, metal to semiconductor transition, resistivity

INTRODUCTION

Currently there is enormous interest in layered magnetic films that may be due to the fact that layering can be used for tuning the properties or to obtain properties which were not characteristic of their bulk forms. For practical reasons, the present study is restricted to the study of a simple structure consisting of two magnetic layers separated by a layer of nonmagnetic material. Very extensive experimental and theoretical investigations on exchange coupling (Kowalewski et al., 1997; Johnson et al., 1992; Egelhoff Jr. and Kief, 1992a) and magneto-optical kerr-effect (Heinrich et al., 1993; Egelhoff Jr. and Kief, 1992b) have been reported on some of these kinds of structures. In some studies, chromium (Cr) spacer instead of copper like metal has been used and investigated the effects of interface roughness (Kumar and Gupta, 2005; Kholin et al., 2006), magnetic and electronic structures (Botana et al., 2008). An anomalous behavior of low

²H.P.S. Kalkhora, Basavakalyan (Tq), Bidar (Dt), India

temperature resistivity has been observed in the structure, Co/M/Co (M = Cr or Cr/Ag or Ag/Cr) (Aliev et al., 1998). The effect of Cu interlayer on grain size and stress has been investigated in sputtered Fe/Cu multilayers (Shamsutdinov et al., 2006). The structural properties were studied for Fe/Cu multilayers as a function of Fe layer thickness (El Khiraoui et al., 2008). Some of these studies were aimed at optimizing the planar structure of (111) Au/Co/Cu trilayers (Kumah et al., 2007). The detailed studies of structure, surface morphology and low temperature electrical properties of Ni/Al/Ni sandwiches have not been reported so far. Hydrogen doping in ZnO has the potential to reveal interesting electrical and optical properties because of its tendency to form easy bonding with charged ions (Singh et al., 2013). Pure semiconducting behavior has been observed in oxidized Ni films (Sadashivaiah et al., 2011) and a sign for metal to semiconductor transition has been noticed in Pb film (Manjunath et al., 2013) at low temperature. Metallic behavior of electrical conductivity at low temperature has been detected in Fe/Cu/Fe sandwiched films (Sadashivaiah et al., 2010). In the present study, we report investigations on structural and electrical properties of Ni/Al/Ni films for different Al spacer layer thicknesses. The layer structure of these films are, (Ni(100 nm)/Al(t)/Ni(100 nm)); t = 10, 20, 30, 40, 50, 60, 70, 80, 90 and $100 \, \mathrm{nm}$.

MATERIALS AND METHODS

The sandwich films, (Ni/Al/Ni) were prepared using electron beam gun and thermal evaporation techniques at a pressure 7×10⁻⁶ mbar and temperature 200°C. The films were deposited onto the well cleaned glass substrates held at a temperature of 473 K. The nickel layers were deposited by evaporating the nickel source from a molybdenum crucible using electron beam gun technique, where as aluminum layers were deposited by thermally evaporating the source from a tungsten filament. The thickness of the layers was measured during deposition using quartz crystal thickness monitor. The films were annealed to room temperature in the vacuum chamber and were subjected to XRD studies in Brucker-D8 advance diffractometer with Cu-Kα radiation of 1.5406 Å wavelength. Electrical resistivity was measured by following four point method in an Oxford Instruments make resistivity setup in the temperature range from 5 to 300 K.

RESULTS AND DISCUSSION

X-Ray Diffraction (XRD) studies: The complete XRD spectrum for NAN1 film and Gaussian fit for the peak are shown in Fig. 1a and b, respectively. Similar spectra were recorded for all the films. The spectra consist of single peak that could be due to the intermixing of the constituent layers i.e., Ni and Al. This is evident from the peak positions of different films which lie between $2\theta = 44.29^{\circ}$ and 44.61° (Table 1). These peak positions do not correspond to either fcc Ni(111) or fcc Al(200). Peak position shifted slightly towards higher angle as the interfacer layer thickness increased. The average grain sizes were estimated using Scherrer's equation (Cullity, 1956):

$$D = (0.9\lambda)/(B \cos \theta_{D})$$

where, D defines the grain size, B the angular width in terms of 2θ , θ_B the Bragg angle and λ the wavelength of the radiation. The interplanar spacing of the films were calculated using the relation, $d = \lambda I (2 \sin \theta_B)$.

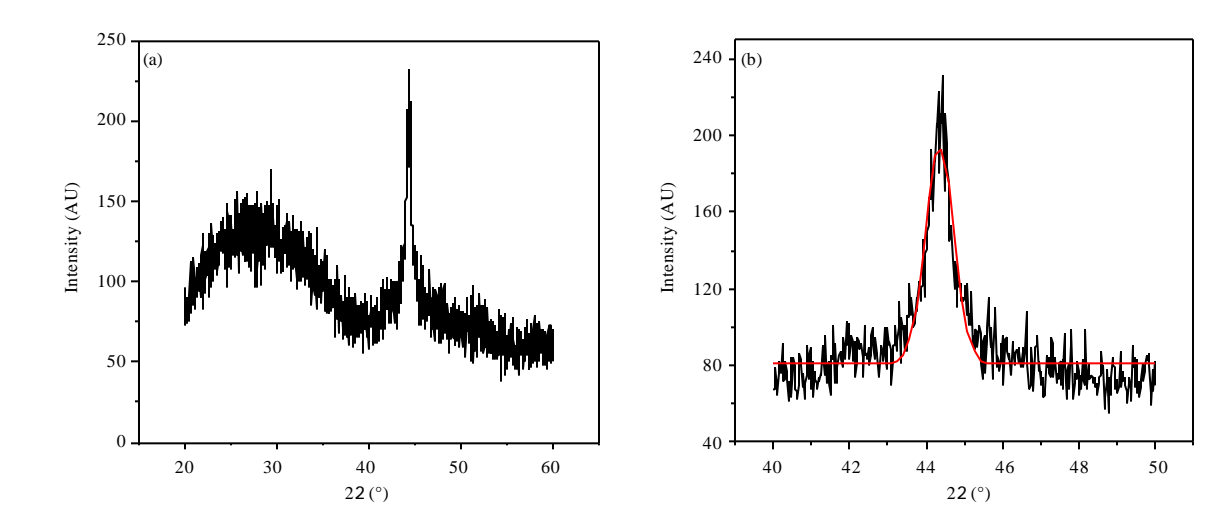


Fig. 1(a-b): (a) XRD spectra for NAN1 film and (b) Spectra around the peak position. The solid line is a Gaussian fit to the peak

Table 1: Parameters	extracted from	YRD enactra	for NAN	candwiched filme

Film	Thickness of Al, t (nm)	Peak position 2θ (Å)	Peak width (Å)	Grain size, D (nm)	Interplanar spacing, d (Å)
NAN1	10	44.359	0.754	11.37	2.040
NAN2	20	44.346	0.945	9.077	2.041
NAN3	30	44.294	0.685	12.51	2.043
NAN4	40	44.374	0.756	11.35	2.040
NAN5	50	44.392	0.694	12.37	2.039
NAN6	60	44.516	0.698	12.29	2.033
NAN7	70	44.491	0.690	12.44	2.034
NAN8	80	44.524	0.798	10.76	2.033
NAN9	90	44.573	0.662	12.96	2.031
NAN10	100	44.610	0.638	13.47	2.029

The structure of the spectra around the peak for all the films have been analyzed and the grain sizes and interplanar spacing were determined (Table 1). These grain sizes obtained are of only few nanometers indicating that the present films are nanocrystalline in nature. The interplanar spacing is lying between 2.029 and 2.043 Å. The measured peak widths are in the range of 0.638 and 0.945 Å. This reveals that the microstructure of the films slightly differs from film to film.

Electrical conductivity: The measured temperature variation of resistivity of all the present films revealed the following information.

- The films NAN1, NAN3 and NAN7 behaved like semiconductors
- Remaining all the seven films exhibited Metal to Semiconductor Transition (MST)

The MST transition temperatures, Tc, are shown in Table 2. Typical plots of temperature variation of ρ for NAN1, NAN4 and NAN10 films are depicted in Fig. 2. From the Fig. 2, it can be seen that in the entire experimental range of temperature NAN1 film behave like a semiconductor.

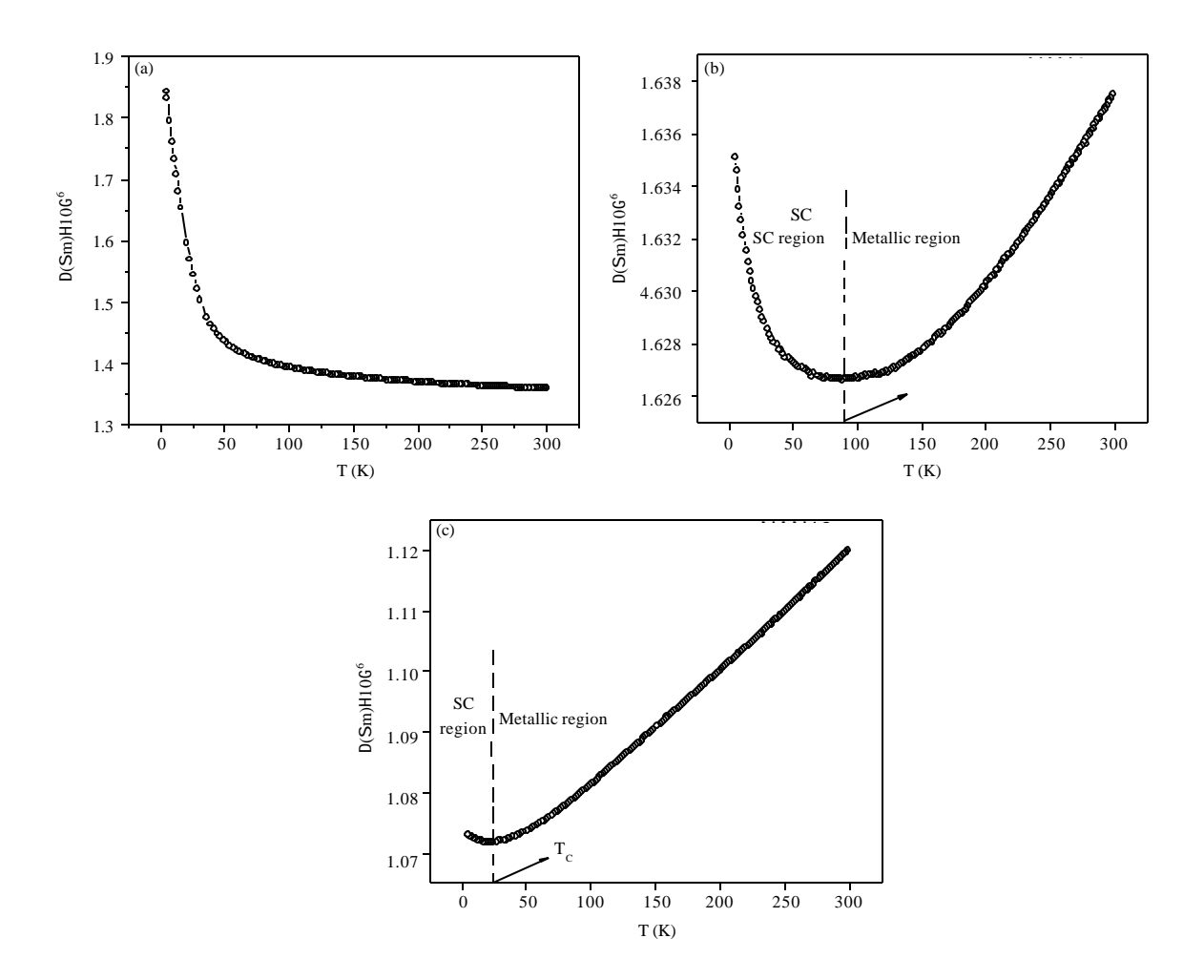


Fig. 2(a-c): Temperature variation of resistivity of (a) NAN1, (b) NAN4 and (c) NAN10

Table 2: MST transition temperatures, Tc of NAN sandwich films

Films	NAN2	NAN4	NAN5	NAN6	NAN8	NAN9	NAN10
T _C (K)	41.12	88.24	80.69	13.96	36.53	24.36	21.43

That is, its resisitivity decreases continuously with increasing temperature. NAN3 and NAN7 films behaved exactly in the same fashion. NAN4 film exhibited metal to semiconductor transition measuring minimum resitivity at transition temperature, Tc. Transition temperature did not vary systematically with interfacer layer thickness as can be seen in Table 2. NAN5 film produced exactly the same type of ρ vs. T spectrum. Whereas, NAN10 film along with NAN2, NAN6, NAN8 and NAN9 measured a short tail on the semiconducting side although MST is quite evident in these film also.

Resistivity variation of NAN1, NAN3 and NAN7 films: Resistivity of NAN1, NAN3 and NAN7 films are in the order of 10^{-6} Ω m. The room temperature conductivity of these films are in agreement with Nio thin film (Hakim *et al.*, 2009) and higher than that of thick Nio films and Nio nano crystals (Makhlouf, 2008; Makhlouf *et al.*, 2009). Resistivity of these three films decreased

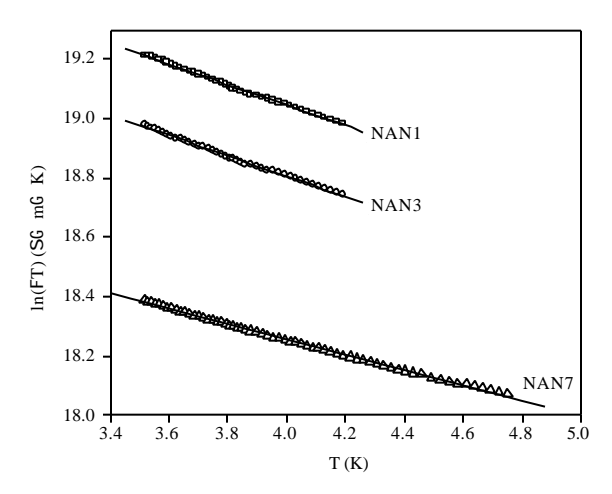


Fig. 3: Plots of $\ln(\sigma T)$ vs. (1/T) for NAN1, NAN3 and NAN7 films for $T>\theta_D$. Solid lines are the linear fits to the data

Table 3: Activation energy, ΔE and density of states, $N(E_F)$ determined from Mott's and Greaves model fits

		Mott's VRH	Greaves VRH
Film	Mott's SPH $\Delta E \text{ (meV)}$	$N(E_F) \; (eV^{-1} cm^{-3})$	$N(E_F)(eV^{-1}cm^{-3})$
NAN1	23.80	2.094×10^{27}	2.446×10^{22}
NAN3	23.29	$2.106\!\! imes\!10^{33}$	5.666×10^{22}
NAN7	23.80	$9.480\!\! imes\!10^{29}$	4.975×10^{26}

continuously with increase in temperature resembling seminconductor behavior. The conducitivity data of these films has been analysed using Mott's small polaron hopping and variable range hopping models due to Mott's and Greaves. For higher temperature, Mott's SPH model gave an expression for condictivity as (Eq. 1):

$$\sigma = (\sigma_0/T)\exp(-\Delta E/k_BT) \tag{1}$$

where, ΔE is the activation energy and σ_0 the pre-exponential factor (Mott, 1968). The plots of $\ln(\sigma T)$ versus (1/T) for these three films are shown in Fig. 3. The least square linear lines were fit to the data for temperatures above θ_D , where θ_D is the Debye's temperature below which the data deviates from linearity. From the slopes, the activation energy, ΔE , was determined and tabulated in Table 3. These activation energy values are smaller than that reported for NiO films and nanocrystals (Hakim *et al.*, 2009; Makhlouf, 2008; Makhlouf *et al.*, 2009).

For the data below θ_D , the Variable-Range Hopping (VRH) models due to Mott (Mott, 1969) and Greave (Greaves, 1973) have been applied. In Mott's VRH model, the conduction is based on a single optical phonon approach and the conductivity is expressed as in Eq. 2:

$$\sigma = A \exp\left(-T_0/T\right)^{1/4} \tag{2}$$

where, $T_0 = 256 (2\alpha^3/9\pi K_BN(E_F))$ and $A = (e^2/2(8\pi)^{1/2}) v_0 (N(E_F)/\alpha KBT)^{1/2}$.

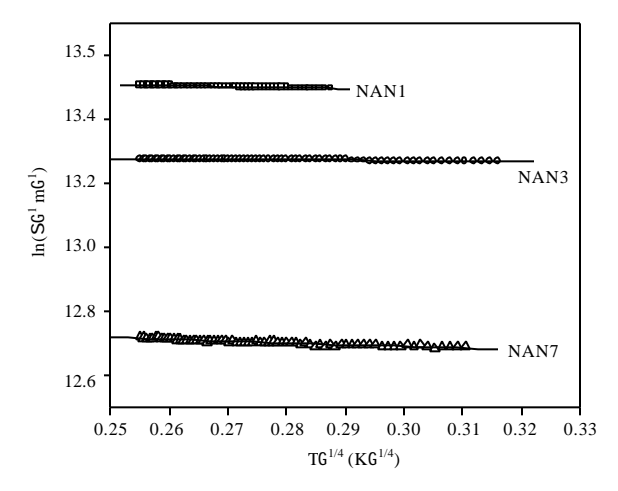


Fig. 4: Plots of $\ln(\sigma)$ vs. $T^{-1/4}$ for NAN1, NAN3 and NAN7 films as per Mott's VRH model. Solid lines are the linear fits for $T < (\theta_D)$

Where $N(E_F)$ is the density of states at the Fermi level. The constants A and T_0 are obtained from the $\ln(\sigma)$ versus $T^{-1/4}$ plots as shown in Fig. 4. Only part of the data below θ_D for which the Motts VRH model fit was in good agreement, is only shown in Fig. 4. It is commonly held that much use of the exponent T_0 has been made to extract values of $N(E_F)$, given assuming value for $\alpha = 10 \text{ nm}^{-1}$ (Elliot, 1984; El-Desoky, 2003). The $N(E_F)$ values obtained are shown in Table 3. These $N(E_F)$ values are much higher than that quoted for NiO nanocrystals (Makhlouf *et al.*, 2009).

The data deviated from Mott's VRH has been considered under Greaves VRH model (Greaves, 1973).

According to this model the conductivity is given by Eq. 3:

$$\sigma T^{1/2} = \text{Bexp}(-T_0/T)^{1/4}$$
 (3)

Where:

$$T_0 = (2.1)^4 [\alpha^3 / k_B N(E_F)]$$

The Greaves plots of $\ln(\sigma T^{1/2})$ versus $T^{-1/4}$ are shown in Fig. 5. From the fit parameters of B and T_0 , the density of states $N(E_F)$ due to Greaves model were estimated and tabulated in Table 3. Both the VRH models appear to fit well with the data in certain range of temperature. However, $N(E_F)$ values derived from them are high compared to that of the reported values for other thin films (Greaves, 1973). It can therefore be concluded that the conductivity of the present films at very low temperatures cannot be satisfactorily explained using Mott's and Greaves VRH models.

Activation energy of all the three films is of the same size approximately. This means that interfacer layer thickness do not affect significantly the activation of conduction process.

Resistivity variation of NAN2, NAN4, NAN5, NAN6, NAN8, NAN9 and NAN10 films: The films NAN2, NAN4, NAN5, NAN6, NAN8, NAN9 and NAN10 showed Metal to Semiconductor Transition (MST). Of these, NAN4 and NAN5 films have exhibited extended tails on either sides

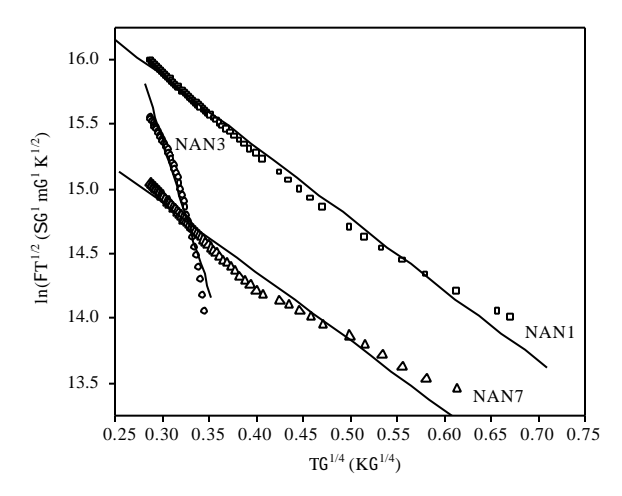


Fig. 5: Plots of $\ln(\sigma T^{1/2})$ vs. $T^{-1/4}$ for the films as per Greaves VRH model. Solid lines are the liner fits to the data

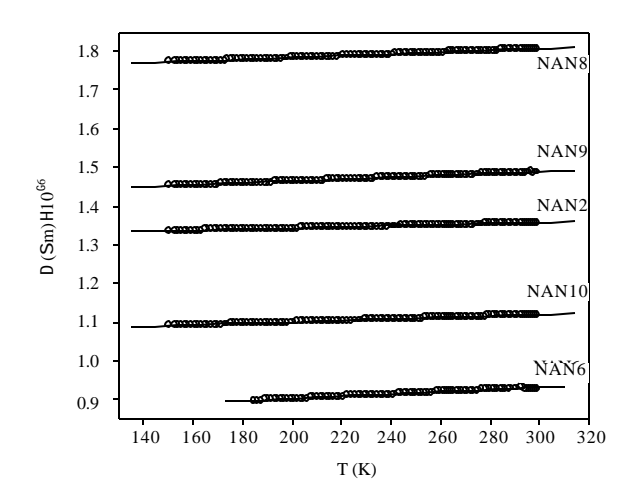


Fig. 6: Plots of ρ vs T for NAN2, NAN6, NAN8, NAN9 and NAN10 films for T>150 K. The lines drawn are the linear fits to the data as per Matheissen's rule

Table 4: Temperature coefficient of resistance, TCR of NAN2, NAN6, NAN8, NAN9 and NAN10 films

Films	NAN2	NAN6	NAN8	NAN9	NAN10
$TCR \times 10^{-4} (K^{-1})$	1.050	2.323	1.307	1.644	1.755

of the transition temperature. Hence, these films have been considered separately for analysis. Other films which have got only short tails on semiconducting side have been considered for analysis under one group. Resistance varied linearly with temperature for NAN2, NAN6, NAN8, NAN9 and NAN10 films for temperature above 150K (Fig. 6). Temperature coefficient of resistance TCR = $(d\rho/dT)/\rho_{300K}$ has been determined and recorded in Table 4. TCR values are positive and are of the order 10^{-4} K⁻¹. Further, linear variation of resistivity with temperature above 150 K is in agreement with Matheissen's rule. According to Matheissen's rule, at high temperature electron-phonon interaction dominates over electron-electron and electron-impurity scattering. Then, resistivity varies linearly with temperature. For T<150K, several attempts have been made

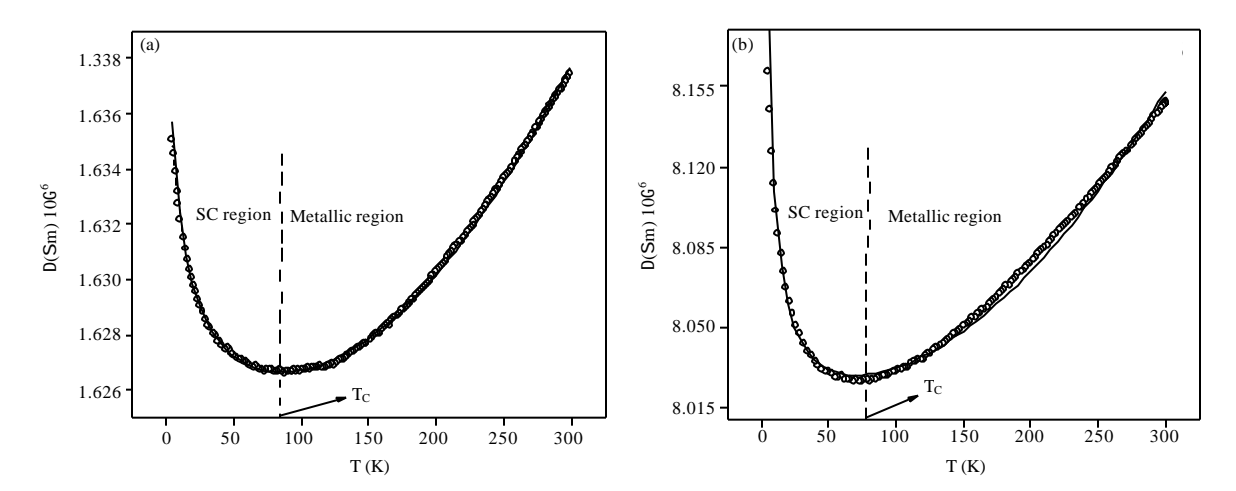


Fig. 7: ρ vs. T for (a) NAN4 and (b) NAN5 films. Solid lines are the best fits to Eq. 4

Table 5: Values of the fit parameters of Eq. 4 to the $\rho(T)$ data on NAN4 and NAN5 films

Sample	$\sigma_0 (\Omega m)^{-1}$	a_1	P	a_2	b
NAN4	1.14×10^{-8}	33.5	0.5	1.62	1.67×10 ⁻⁷
NAN5	1.23×10^{-8}	1.2	1.8	8.00	1.61×10^{-6}

to fit the data to $\rho = AT^5$, as dedicated by Matheissen's rule and also to Arrhenius expression $\rho = \rho_0 \exp(E/K_BT)$. But no good fits were achieved, implying that for these films, different theoretical treatment is required to understand resistivity below 150 K.

Resistivity variation of NAN4 and NAN5 films: The $\rho(T)$ data on NAN4 and NAN5 films hints at the presence of competing mechanisms operating in these samples. The negative Temperature Coefficient of Resistance (TCR) below T_C indicates localization of electrons and the positive TCR above T_C suggests delocalization of electrons (Pradhan et al., 2007). The delocalization of electrons leads to metallic conductivity which is a characteristic feature of degenerate semiconductor (Shimakawa et al., 1999). The metal-semiconductor transition can be explained using a view proposed for conduction in disordered matter (Lee and Ramakrishnan, 1985) where, the minima in the $\rho(T)$ curve has been accounted for Quantum Correction (QC) terms in the conductivity expression. This view was developed based on Boltzmann semiclassical approach. The QC terms come from weak localization and Coulomb interaction effects that are related to structural disorder (Lee and Ramakrishnan, 1985). The localization effects have already been considered to interpret the MST observed in various oxides such as RuO₂ (Herranz et al., 2004), ZnO:Ga (Pradhan et al., 2007) and undoped ZnO (Nistor et al., 2009). According to Lee and Ramakrishnan (1985), the resistivity including the QC can be expressed as Eq. 4:

$$\rho = 1/(\sigma_0 + a_1 T^{p/2} + a_2 T^{1/2}) + (bT^2)$$
(4)

where, ρ_0 (=1/ σ_0) is the residual resistivity. The second term in the denominator corresponds to weak localization and the third term corresponds to Coulomb interaction effects. Equation 4 was fit to the data of NAN4 and NAN5 as shown in Fig. 7. The best fit parameters obtained are recorded in Table 5. Form Table 5, it can be seen that in case of NAN4, $a_1>a_2$ and in the case of NAN5, $a_1<a_2$.

These indicate that within QC, weak localization effect dominates over coulomb interaction in NAN4 film and reverse is the case in NAN5 film. The values of P for NAN4 and NAN5 were determined to be 0.5 and 1.8, respectively which correspond to electron-phonon interaction at weak localization sites (Shimakawa *et al.*, 1999).

CONCLUSION

- A set of sandwich films, Ni(100 nm)/Al(t)/Ni(200 nm); t =10-10 nm were deposited by thermal
 and electron beam gun methods at 473 K under high vacuum conditions. The structure and
 grain sizes were probed through X-Ray Diffraction (XRD) studies
- Low temperature electrical resistivity has been measured. Temperature dependence of resitivity showed complete semiconducting behavior for the films NAN1, NAN3 and NAN7. The data of these films has been analyzed in the light of Mott's small polaron hopping model and variable range hopping models due to Mott and Greave
- Resistivity data of NAN2, NAN6, NAN8, NAN9 and NAN10 films obeyed Matheissen's rule of linear relation between ρ and T at high temperature
- Data on NAN4 and NAN5 films has been fit to resistivity expression which incorporates
 quantum correction in to it. The best fits were achieved and the coefficients corresponding to
 electron localization and coulomb interaction effects have been determined

It is for the first time that sandwiched films of the present type have been found to be exhibiting MST and the data has been thoroughly analyzed taking various effects into account.

ACKNOWLEDGMENTS

Authors acknowledge the financial support received from UGC, New Delhi in the form a Major Research Project sanctioned to Prof. T. Sankarappa. Also, Prof. T. Sankarappa acknowledges the rigorous research training that he received from Mike Springford and Dr. P.J. Meeson at H.H. Wills Physics Laboratory, University of Bristol, UK.

REFERENCES

- Aliev, F.G., V.V. Moshchalkov and Y. Bruynseraede, 1998. Anomalous low-temperature resistivity of metallic trilayers: Possible evidence for electron scattering on symmetrical two-level systems. Phys. Rev. B, 58: 3625-3628.
- Botana, J., M. Pereiro, D. Baldomir, H. Kobayashi and J.E. Arias, 2008. Magnetic and electronic structure of nFe/3Cr/nFe slabs (n = 1→6). Thin Solid Films, 516: 5144-5149.
- Cullity, B.D., 1956. Elements of X-Ray Diffraction. Addison-Wesley Inc., Massachusetts, USA.
- Egelhoff Jr., W.F. and M.T. Kief, 1992a. Antiferromagnetic coupling in Fe/Cu/Fe and Co/Cu/Co multilayers on Cu(III). Phys. Rev. B, 45: 7795-7804.
- Egelhoff Jr. W.F. and M.T. Kief, 1992b. Fe/Cu/Fe and Co/Cu/Co multilayers on Cu(III): The absence of oscillatory antiferromagnetic coupling. IEEE Trans. Magnetics, 28: 2742-2744.
- El Khiraoui, S., M. Sajieddine, M. Hehn, S. Robert and O. Lenoble *et al.*, 2008. Magnetic studies of Fe/Cu multilayers. Phys. B: Condensed Matter, 403: 2509-2514.
- El-Desoky, M.M., 2003. Small polaron transport in V_2O_5 -NiO-TeO $_2$ glasses. J. Mater. Sci. Mater. Electron., 14: 215-221.
- Elliot, S.R., 1984. Physics of Amorphous Materials. Longman Inc., New York, USA.

Asian J. Applied Sci., 7 (8): 685-695, 2014

- Greaves, G.N., 1973. Small polaron conduction in V₂O₅ P₂O₅ glasses. J. Non-Cryst. Solids, 11: 427-446.
- Hakim, A., J. Hossain and A.K. Khan, 2009. Temperature effect on the electrical properties of undoped Nio thin films. Renewable Energy, 34: 2625-2629.
- Heinrich, B., Z. Celinski, J.F. Cochran, A.S. Arrott, K. Myrtle and S.T. Purcell, 1993. Bilinear and biquadratic exchange coupling in bcc Fe/Cu/Fe trilayers: Ferromagnetic-resonance and surface magneto-optical Kerr-effect studies. Phys. Rev. B., 47: 5077-5089.
- Herranz, G., F. Sanchez, B. Martinez, J. Fontcuberta and M.V. Garcia-Cuenca *et al.*, 2004. Weak localization effects in some metallic perovskites. Eur. Phys. J. B Condensed Matter Complex Syst., 40: 439-444.
- Johnson, M.T., S.T. Purcell, N.W.E. McGee, R. Coehoorn, J. de Stegge and W. Hoving, 1992. Structural dependence of the oscillatory exchange interaction across Cu layers. Phys. Rev. Lett., 68: 2688-2691.
- Kholin, D.I., A.B. Drovosekov, S.O. Demokritov, M. Rickart and N.M. Kreines, 2006. Noncollinear interlayer exchange in Fe/Cr/Fe magnetic structures with different interface roughnesses. Phys. Metals Metallography, 101: S67-S69.
- Kowalewski, M., B. Heinrich, J.F. Cochran and P.J. Schurer, 1997. Studies of interlayer exchange coupling in Fe/Cu/Fe ultrathin heterostructures. J. Applied Phys., 81: 3904-3906.
- Kumah, D.P., A. Cebollada, C. Clavero, J.R. Skuza, R.A. Lukaszew and R. Clarke, 2007. Optimizing the planar structure of (111) Au/Co/Au trilayers. J. Phys. D: Applied Phys., 40: 2699-2704.
- Kumar, D. and A. Gupta, 2005. Effects of interface roughness on interlayer coupling in Fe/Cr/Fe structure. Hyperfine Interact., 160: 165-172.
- Lee, P.A. and T.V. Ramakrishnan, 1985. Disordered electronic systems. Rev. Modern Phys., 57: 287-295.
- Makhlouf, S.A., 2008. Electrical properties of nio films obtained by high-temperature oxidation of nickel. Thin Solid Films, 516: 3112-3116.
- Makhlouf, S.A., M.A. Kassem and M.A. Abdel-Rahim, 2009. Particle size-dependent electrical properties of nanocrystalline NiO. J. Matter. Sci., 44: 3438-3444.
- Manjunath, A.W., T. Sankarappa, R. Ramanna, J.S. Ashwajeet, T. Sujatha and P. Sarvanan, 2013. Low temperature electrical resistivity studies in lead thin films. J. Nano-Electron. Phys., Vol. 5.
- Mott, N.F., 1968. Conduction in glasses containing transition metal ions. J. Non-Crystal. Solids, 1: 1-17.
- Mott, N.F., 1969. Conduction in non-crystalline materials III. Localized states in a pseudogap and near extremities of conduction and valence bands. Philos. Mag., 19: 835-852.
- Nistor, M., F. Gherendi, N.B. Mandache, C. Hebert, J. Perriere and W. Seiler, 2009. Metal-semiconductor transition in epitaxial ZnO thin films. J. Applied Phys., Vol. 106. 10.1063/1.3259412
- Pradhan, A.K., L. Douglas, H. Mustafa, R. Mundle, D. Hunter and C.E. Bonner, 2007. Pulsed-laser deposited Er: ZnO films for 1.54 im emission. Applied Phys. Lett., Vol. 90. 10.1063/1.2560764
- Sadashivaiah, P.J., T. Sankarappa and T. Sujatha, 2011. Magnetic and low temperature conductivity studies in oxdised nano films. J. Nano-Electron. Phys., 3: 43-54.

Asian J. Applied Sci., 7 (8): 685-695, 2014

- Sadashivaiah, P.J., T. Sankarappa, T. Sujatha, Santoshkumar, R. Rawat, P. Sarvanan and A.K. Bhatnagar, 2010. Structural, magnetic and electrical properties of Fe/Cu/Fe films. Vacuum, 85: 466-473.
- Shamsutdinov, N.R., A.J. Bottger and F.D. Tichelaar, 2006. The effect of Cu interlayers on grain size and stress in sputtered Fe-Cu multilayered thin films. Scripta Materialia, 54: 1727-1732.
- Shimakawa, K., S. Narushima, H. Hosono and H. Kawazoe, 1999. Electronic transport in degenerate amorphous oxide semiconductors. Philos. Mag. Lett., 79: 755-761.
- Singh, A., S. Chaudhary and D.K. Pandya, 2013. Hydrogen incorporation induced metal-semiconductor transition in ZnO: H thin films sputtered at room temperature. Applied Phys. Lett., 102: 172106-172106-5.